Combination of photodynamic therapy and gene silencing achieved through the hierarchical self-assembly of porphyrin-siRNA complexes

Nabila Laroui, Maëva Coste, Laure Lichon, Yannick Bessin, Magali Gary-Bobo, Geneviève Pratviel, Colin Bonduelle, Nadir Bettache, Sébastien Ulrich

▶ **To cite this version:**

Nabila Laroui, Maëva Coste, Laure Lichon, Yannick Bessin, Magali Gary-Bobo, et al.. Combination of photodynamic therapy and gene silencing achieved through the hierarchical self-assembly of porphyrin-siRNA complexes. International Journal of Pharmaceutics, 2019, 569, pp.118585. 10.1016/j.ijpharm.2019.118585 . hal-02322136

HAL Id: hal-02322136
https://hal.science/hal-02322136v1

Submitted on 18 Nov 2020

HAL is a multi-disciplinary open access archive for the deposit and dissemination of scientific research documents, whether they are published or not. The documents may come from teaching and research institutions in France or abroad, or from public or private research centers.

L'archive ouverte pluridisciplinaire **HAL**, est destinée au dépôt et à la diffusion de documents scientifiques de niveau recherche, publiés ou non, émanant des établissements d'enseignement et de recherche français ou étrangers, des laboratoires publics ou privés.

International Journal of Pharmaceutics
Full Length Manuscript

Combination of photodynamic therapy and gene silencing achieved through the hierarchical self-assembly of porphyrin-siRNA complexes

Nabila Laroui,[a] Maëva Coste,[a] Laure Lichon,[a] Yannick Bessin,[a] Magali Gary-Bobo,[a] Geneviève Pratviel,[b] Colin Bonduelle,[b,c] Nadir Bettache,[a]* Sébastien Ulrich[a]*

[a] IBMM, Université de Montpellier, CNRS, ENSCM, Montpellier, France
[b] CNRS, LCC (Laboratoire de Chimie de Coordination, UPR8241), Université de Toulouse, 205 route de Narbonne, F-31077 Toulouse, France
[c] Laboratoire de Chimie des Polymères Organiques, Université de Bordeaux/IPB, ENSCBP, 16 avenue Pey Berland, 33607 Pessac Cedex, France
E-mail: nadir.bettache@umontpellier.fr; Sebastien.Ulrich@enscm.fr

Abstract

In this work, we implemented a supramolecular approach in order to combine photodynamic therapy (PDT) with gene therapy. We made use of a simple cationic guanidylated porphyrin (**H_2-PG**) with the hypothesis that porphyrin aggregates should be capable of complexing siRNA through multivalent interactions and thus contribute to its intracellular delivery, while remaining active photosensitizers for PDT. The PDT effect of **H_2-PG** was shown by incubating human breast cancer cells (MDA-MB-231) with **H_2-PG** followed by light-irradiation at 405 nm. On the other hand, while siRNA do not enter cells alone, we showed, by fluorescence confocal microscopy and flow cytometry, that **H_2-PG** promotes the internalization of Atto-488 siRNA. Finally, studying the combined PDT and delivery of siRNA directed against inhibitory apoptotic protein (IAP) family, we found an additive effect of the two therapies, thereby demonstrating that **H_2-PG** is capable of acting both as a photosensitizer and supramolecular siRNA vector.

Keywords

Combination therapy; photodynamic therapy; gene therapy; supramolecular self-assembly; porphyrin; siRNA

Graphical abstract

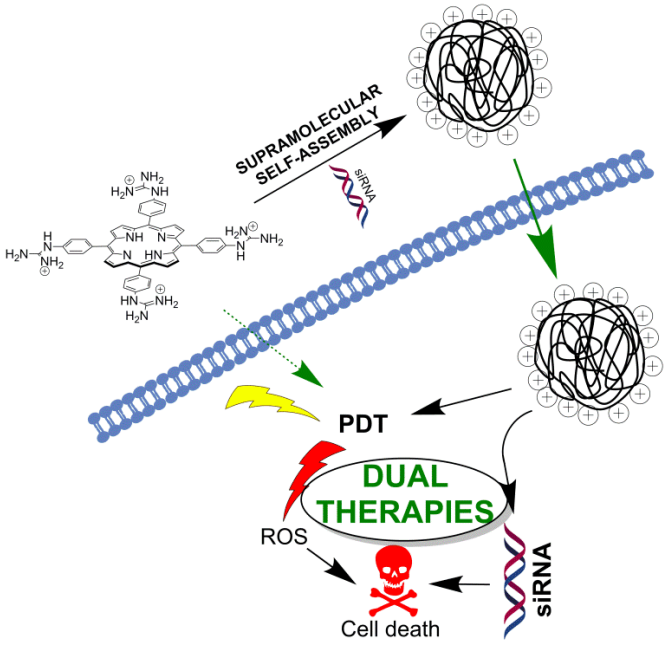

Introduction

Cancer is an extremely complex disease which remain a major threat to human health.[1] The current therapeutic arsenal based on chemotherapy and radiotherapy generates many side effects due to off target interactions and in some cases shows limited efficacy. Therefore, combination therapies are attracting growing interest in nanomedecine.[2] It is expected that, by attacking several pathways at once, one would enhance the overall effect and limit resistance. Additive effects of the two treatments, or even synergistic effects, whereby one treatment amplifies the effect of the second one, are actively pursued. In this context, the combination of PhotoDynamic Therapy (PDT) with gene therapy can be particularly promising since mechanisms of photochemical internalization[3] and/or photoinduced endosomal release[4] could lead to such synergistic effects.

Gene therapy using siRNA to knockdown the expression of a target gene has become an effective way for gene silencing approaches.[5-7] However, several limitations remain in the clinical applications of RNA interference such as poor distribution and high instability of siRNA in the body fluid as it is degraded by ribonucleases. Moreover, the issue of intracellular delivery remains central in this area.

PDT is the fourth strategy used against cancer in the clinic (after surgery, chemo- and radio-therapy) which is minimally invasive and features high spatio-temporal specificity.[8] PDT requires PhotoSensitizers (PS), such as porphyrins,[9, 10] which are associated with light at an appropriate wavelength to generate Reactive Oxygen Species (ROS), including singlet oxygen ($^1O_2$), to induce cell death and tissue destruction through apoptosis or necrosis pathways.[8, 11, 12] The mechanism of action of PDT is based on the light-activation of PS and subsequent energy transfer to the surrounded molecular oxygen (O_2) which leads to the production of ROS. The current developments of PDT include the design of smart photosensitizers[13] among which supramolecular photosensitizers are emerging.[14]

Only a few examples of studies combining PDT and gene delivery have been documented, using covalent siRNA vector-photosensitizer conjugates,[15] porous organo-silica nanoparticles,[16] dendrimers,[17] polydiacetylene micellar nanocarriers,[18] and polyelectrolytes.[19]

In this work, we pursued a supramolecular approach to combine PDT with gene therapy using a simple cationic porphyrin as a dual photosensitizer and supramolecular siRNA vector. Our rational was that porphyrins are well-known PS for PDT, and at the same time they are prominent building blocks for the

generation of supramolecular self-assemblies.[20] Therefore, we thought of using cationic porphyrins for their role as PS and for generating multi-cationic porphyrin aggregates that would promote the multivalent complexation and intracellular delivery of siRNA.[21] Based upon our previous works on porphyrin-based G-quadruplex DNA ligand[22] and DNA-templated self-assembly of aromatic guanidiniums,[23, 24] we selected meso-5,10,15,20-tetrakis(4-guanidinophenyl)porphyrin tetrahydrochloride (**H_2-PG**) for this study. **H_2-PG** is water-soluble and has a Soret band centered at 415 nm (ε = 430000 $M^{-1}cm^{-1}$). The aromatic guanidiniums have pKa = 9.8 while the inner core has a pKa = 3.8, therefore **H_2-PG** is considered a tetracationic species.

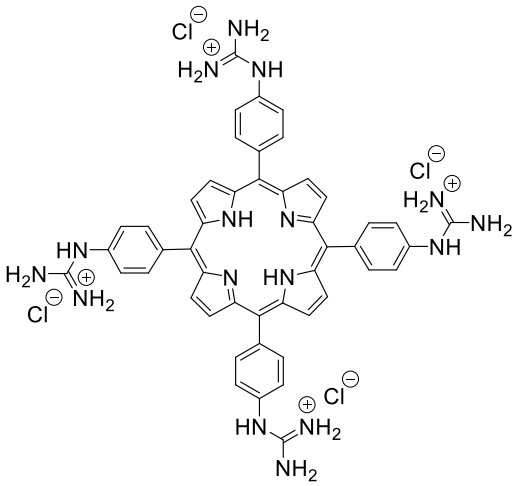

Figure 1. Chemical structure of **H_2-PG**.

Material and methods

Material: **H_2-PG** was synthesized as previously described.[22, 25] The oligonucleotides dT_{10} and dT_{40} were purchased from Eurogentec as HPLC-RP purified (Ultrapure Gold, >95% purity) in dried format. Calf thymus DNA (CT-DNA) was purchased from Sigma-Aldrich. The siRNA inhibitor apoptotic protein (siIAP) targeting sequence (sense: 5'-CUAGGAGACAGUCCUAUUCdTdT-3' and anti-sense 5'-GAAUAGGACUGUCUCCUAGdTdT-3'), the control siRNA labeled with Atto-488 (Atto-488-siCtrl) (sense: 5'-CGUACGCGGAAUACUUCGAdTdT-3' and anti-sense 5'-UCGAAGUAUUCCGCGUACGdTdT-3'), the siRNA without biological activity, used as control (siCtrl) (sense: 5'-CGUACGCGGAAUACUUCGAdTdT-3' and anti-sense 5'-UCGAAGUAUUCCGCGUACGdTdT-3') and the siRNA scramble (siScr) (Sense: 5'-GAAUCCUCGGUCGAUAUCAdTdT 3' and anti-sense: 5'- GGCCAUUAUCGCGUAAGAUdTdT 3') were purchased from Eurogentec (Serring, Belgium). Lipofectamine RNAiMAX was purchased from Invitrogen (USA). The MTT (3-(4,5-dimethyl-thiazol-2-yl)-2,5-diphenyltetrazolium bromide, a yellow tetrazole) assay kit was purchased from Sigma-Aldrich (Saint-Quentin-Fallavier, France).

UV-Vis absorption spectroscopy: UV-Vis absorption experiments were measured on UV-3100pC UVisco spectrophotometer. Experience with dT_{10}: 20 µL of a stock solution of dT_{10} (10 mM in H_2O), placed in a 1 mm Quartz cuvette (volume completed to 400 µL with H_2O) was titrated by adding aliquots of **H_2-PG** from a stock solution (5 mM in H_2O). Experience with CT-DNA: 2 µL of **H_2-PG** (from a stock solution of 5 mM in H_2O), placed in a 1 mm Quartz cuvette (volume completed to 400 µL with H_2O), was titrated by adding aliquots of CT-DNA from a stock solution of 2 $mg.mL^{-1}$ in H_2O.

Fluorescence spectroscopy: Fluorescence analyses were carried out on an AF-2500 HITACHI fluorescence spectrophotometer. 0.2 µL of **H_2-PG** (from a stock solution of 5 mM in H_2O), placed in a 1 mm Quartz cuvette (volume completed to 400 µL with H_2O), was titrated by adding aliquots of dT_{10} (10 mM stock solution in H_2O). Excitation wavelength: 415 nm.

Circular dichroism spectroscopy: Circular dichroism measurements were recorded using a JASCO J-815 CD Spectrophotometer. The measurements were carried out at 20 °C using a 1 mm quartz cells (Starna

scientific). The spectra were recorded between 220 and 500 nm, with a bandwidth of 1 nm and time per point of 0.5 s. Baseline signals (recorded with water) were subtracted from the CD spectra of the samples. 9.81 µL of dT_{40} (stock solution of 143 µM in H_2O) were placed in the cell, completed with 190 µL of H_2O and then titrated with **H_2-PG** (stock solution of 5 mM in H_2O).

Cell line: MDA-MB 231 human breast cancer cells were purchased from ATCC**.** Cells were grown in phenol red-free F12/ Dulbecco's modified Eagle's medium (DMEM) supplemented with 10% fetal calf serum (FCS)and 1% gentamycin 50 µg.mL^{-1}. The cells were incubated at 37 °C in a humidified atmosphere with 5% CO_2.

Gel electrophoresis with siRNA: Gel retardation assays with siRNA were performed using 10 µL of a 4 µM siCtrl, which were mixed with the appropriate amounts of porphyrins **H_2-PG** (in order to reach the desired N/P ratio[26]) in RNase free water to obtain a final volume of 20 µL. 4 µL of Blue 6X loading dye (Fisher Scientific) was added. Electrophoresis was carried out on a 2% weight/volume agarose gel in TBE (90 mM Tris-borate/2 mM EDTA, pH 8.2) at 50 V for 1 h. siRNA was visualized with GelRedTM nucleic acid gel stain (Interchim, France). The reference for the gel is a 100 bp DNA ladder from Sigma-Aldrich (Saint-Quentin-Fallavier, France). The GelRed-stained siRNA was visualized on an ultraviolet transilluminator (Infinity Gel documentation Imaging, Vilber Lourmat, France).

Dynamic light scattering: Particle size measurements were carried out on a Zetasizer NanoZS (Malvern, United Kingdom) with transparent ZEN0040 disposable micro-cuvette (40 µL) at 25 °C. The **H_2-PG**/siRNA complexes were prepared in glucose 5% at a defined N/P ratio using siCtrl at several concentrations. Measurements were performed immediately after the complexes formation and after 15 min incubation.

Zeta Potential: Zeta Potential analyses were carried out on a MALVERN Zetasizer Nanoseries NANO-ZS instrument. The **H_2-PG**/siRNA complexes were prepared by mixing appropriate amounts of **H_2-PG** and siCtrl to achieve the desired N/P ratio and diluted in glucose 5% and NaCl (5 mM, pH = 7.0) to obtain a final volume of 1 mL. Measurements were performed at 25 °C and were carried out in DTS 1070 zeta potential cells. 3 measurements were made with 12 runs for each.

Imaging: One day prior the experiment, MDA-MB 231 cells were plated onto bottom 8-well on cover glass II (SARSTEDT, Germany) at a density of 1.10^5 cells.cm^{-2}. Adherent cells were then washed once and incubated in 350 µL culture medium containing complex H_2-PG (5 µM)/Atto-488-siCtrl (100 nM) at N/P=5, **H_2-PG** alone, at a concentration of 5 µM, Lipofectamine/Atto-488-siCtrl (50 nM) and siRNA Atto488 alone (100 nM) for 20 h. Adherent cells were washed and loaded with 350 µL of Hoechst 33342 (invitrogen, USA) 1/1000 in culture medium. Prior the observation, cells were washed gently with culture medium, then visualized with a Zeiss LSM780 confocal microscope (Carl Zeiss Microscope, France) at 488 nm for siRNA, 405 nm for **H_2-PG** porphyrins and 360 nm for Hoechst 33342 using bright field at high magnification (63x/1.4 OIL Plan-Apo).

Internalization quantification by FACS: Cells were treated or not with **H_2-PG** (5 µM)/Atto-488-siCtrl (100 nM) at N/P = 5, **H_2-PG** alone, at a concentration of 5 µM, Lipofectamine/Atto-488-siCtrl (50 nM) and siRNA Atto488 alone (100 nM) for 20 h. After treatment, control and treated cells were washed once in cold Phosphate Buffer Saline (PBS), harvested and centrifuged (1300 rpm, 5 min). Cell pellet were resuspended in PBS enriched with $CaCl_2$ + $MgCl_2$+ and stained with propidium iodide (1 µg.mL^{-1}) (Sigma-Aldrich Chimie, Lyon, France), a cell death indicator. Flow cytometric determination of living cells and treated positive cells was done by FACS Gallios Flow Cytometer (Beckman Coulter, France) with a minimum of 5,000 living cells collected. Data were analyzed with Kaluza software.

In vitro **Photo-Induced siRNA Delivery:** The day prior to transfection, 2.10^3 cells were seeded into a 96 well plate in 100 µL complete culture medium and incubated for 24 h. **H_2-PG** at 5 mM in ultrapure water were vortexed for 5 sec and ultrasonically mixed for 15 min. siIAP and siScr at 100 µM in RNase free water were mixed with **H_2-PG** in order to reach the desired N/P. The mixtures freshly prepared were incubated for 15 min at room temperature for pairing. The lipofectamine RNAiMAX was mixed with siIAP (50 nM final

concentration) according to the instructions (0.3 µL of lipofectamine/well for a 96 well plate). Then, cells were incubated overnight with several concentrations of **H_2-PG** alone (5 µM or 25 µM) or paired with siRNA (100 nM or 500 nM). After incubation, the cells were irradiated (or not) with laser at 405 nm (KAMAX, France) for 10 min. Two days after irradiation, MTT assay was performed to evaluate the cell death. Briefly, cells were incubated for 4 h with 0.5 $mg.mL^{-1}$ of MTT in media. The MTT/media solution was then removed and the precipitated crystals were dissolved in EtOH/DMSO (1:1). The absorbance was read at 540 nm.

In-cell ELISA: MDA-MB 231 cell lines (1.10^4 cells/well; 70% confluence) were seeded in a 96 wells plate and incubated overnight at 37 °C in 5% CO_2. Cells were treated with the several conditions as mentioned above then were fixed with PBS-4% PFA for 15 min, washed and blocked with Blocking Solution "BS" for 30 min. Supernatants were then gently aspirated and the primary antibody (Rabbit polyclonal anti-cIAP, GeneTex) diluted 1:1000 in BS/washing buffer "WB" was added and incubated overnight at 4 °C. The reaction was revealed using an anti-Rabbit-peroxidase conjugate (1:400 in WB; 30 min at RT). After three washes with WB, the TMB (3,3',5,5'-tetramethylbenzidine) substrate was added and incubated for 15 min at room temperature protected from light. The reaction was stopped with a TMB STOP solution and plate was read at 450 nm. To account for differences in cell seeding density was normalized to the Janus Green staining dye. Briefly, after the in-cell assay protocol was completed, the plate was washed twice with ultrapure water and Janus Green stain (Thermo Fisher Scientific, Waltham MA, USA) was added (100 µl/well). The plate was incubated for 5 min at RT. Then the dye was removed and after 5 washes, the plate was incubated with 100 µL elution buffer and read at 615 nm. Once normalized, TMB-optical density (OD) values of each sample were subtracted from the mock-treated wells (corrected OD values) and averaged from triplicate wells. Each assay was repeated at least twice.

Results and Discussion

H_2-PG/DNA interactions and mode of binding

Porphyrin can self-associate into supramolecular polymers,[20] but cationic porphyrins are also known to be excellent DNA ligands.[27] Generally speaking, DNA binding can occur according to three different modes (intercalation,[28, 29] groove binding,[30, 31] external binding[23, 24]) and all of them have been reported with cationic porphyrins of different structures varying the position and size of their substituents, and the nature, number and position of positive charges.[27, 32-34] Wishing to explore the specific mode of binding of **H_2-PG**, we studied its interaction with different types of DNA, single- and double-stranded, by UV-Vis, fluorescence, and circular dichroism spectroscopies.

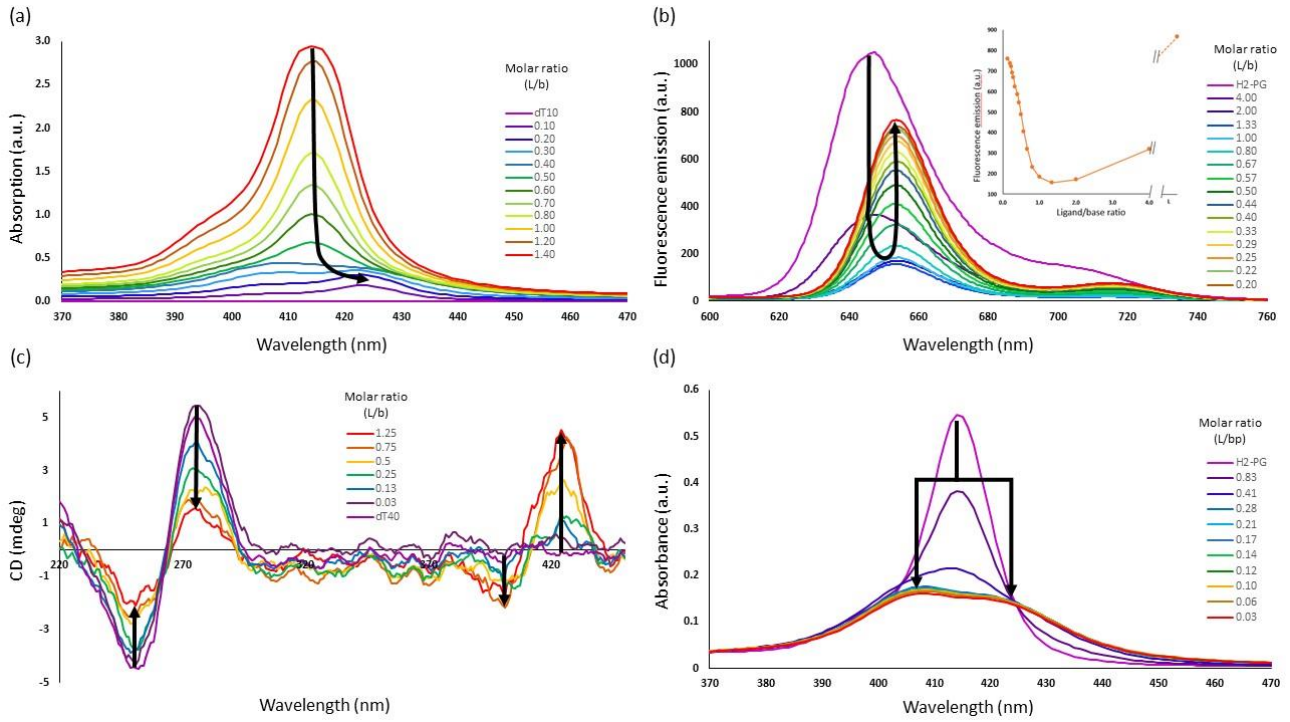

Figure 2. **H_2-PG**/DNA interactions studied by optical spectroscopies. (a) UV-Vis titration of a $ssdT_{10}$ by **H_2-PG**; (b)Fluorescence titration of **H_2-PG** by $ssdT_{10}$ (Inset: fluorescence emission at 655 nm as a function of the **H_2-PG**/nucleobase molar ratio (L/b)); (c) Circular dichroism titration of a solution of $ssdT_{40}$ by **H_2-PG**; (d) UV-Vis titration of **H_2-PG** by CT-DNA. **H_2-PG**/nucleobase molar ratio: L/b. **H_2-PG**/base pair molar ratio (L/bp).

UV-Vis titration using a dT_{10} single-strand DNA (ssDNA) showed hypochromic and bathochromic shifts of the absorbance of **H_2-PG** (Figure 2a). Fluorescence measurements showed a sharp decrease in the fluorescence emission around a ligand/nucleobase ratio of 1-2, with a 10 nm red-shift (Figure 2b). In the presence of a dT_{40} ssDNA, CD spectroscopy revealed the formation of a bisignate ICD signal centered around the Soret band of **H_2-PG** with a zero crossing around 410-415 nm (Figure 2c). Altogether, these results points toward an external binding with DNA-templated self-stacking of **H_2-PG**,[35-37] which we previously reported with ssDNA templates and guanidylated ligands.[23, 24] Indeed, the bisignate signal observed in CD spectroscopy reveals the presence of excitons which result from the close proximity between adjacents **H_2-PG**.[38] Given the fact that ssDNA templates do not offer the possibility for groove binding, we propose that this ssDNA-templated self-assembly involves salt-bridge interactions between guanidinium groups and DNA phophodiesters, and π-stacking of **H_2-PG** into 1D supramolecular polymers. Using longer and double-stranded (ds) DNA (Calf-Thymus DNA, CT-DNA), UV-Vis titration experiments showed the splitting of the Soret band of **H_2-PG** into two separate peaks, one bathochromically- and one hypsochromically-shifted (Figure 2d). This may reveal a more complex situation with long dsDNA templates, compared to ssDNA, which offer multiple modes of binding for the poly-association of **H_2-PG**, including the intercalation described between cationic copper(II) porphyrins and dsRNA.[39]

H_2-PG/siRNA complexation

To demonstrate complexation of siRNA, we assessed **H_2-PG**/siRNA complex formation by agarose shift assay (Figure 3a). This assay was used to follow the complexation state in a charge ratio-dependent manner because siRNA migration into the agarose gel will be prevented by porphyrin interactions. In this experiment we used siCtrl and tested different N/P ratios[26] (2, 5, 10). The results showed clearly no shift of the siRNA at ratio of 2. However, a strong retardation effect was observed with the complete disappearance of the band corresponding to the native siRNA at N/P = 5. In conclusion, agarose gel assay clearly showed that **H_2-PG** does complex siRNA.

Size and ζ-potential determination of H_2-PG/siRNA nanoparticles

The size and zeta potential of **H_2-PG**/siRNA nanoparticles are important for gene delivery in terms of influencing cellular uptake and transfection efficiency. The condensation of siCtrl into nanoparticles, promoted by **H_2-PG**, was studied by dynamic light scattering (DLS) experiments at N/P = 5. Size and homogeneity were determined for each complex (5% glucose, N/P = 5) (Figure 3b). DLS investigations revealed that using a 5 µM concentration of **H_2-PG** leads to small nanoparticles with diameters of 217.2 nm and with polydispersity index (PDI) of 0.324. We have also tested larger concentrations: 25 and 50 µM and we observed the formation of much larger particles (average diameters of 540.2 nm and 449.5 nm respectively, with PDI of 0.506 and 0.234 respectively), unsuitable for cell entry through typical endocytosis pathways. We next evaluated surface charge of nanoparticles by zeta potential (ZP) measurements which revealed a value of 18.5 mV at a concentration of 5 µM and 32.4 mV and 35.2 mV for concentrations of 25 µM and 100 µM, respectively. The complex formed between **H_2-PG** and siRNA remained therefore positively charged, which is an advantage for cell entry.

(a) **(b)**

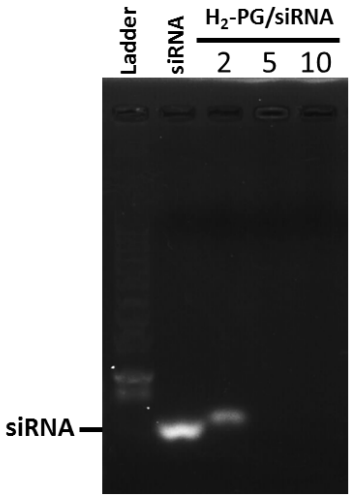

Compounds (concentrations)	SIZE (nm)	PDI*	ζ POTENTIAL (mV)
H_2-PG + siRNA (5 µM)	217.2 ± 26.75	0.324 ± 0.014	+18.5 ± 0.436
H_2-PG + siRNA (25 µM)	540.2 ± 31.91	0.506 ± 0.354	+32.4 ± 5.52
H_2-PG + siRNA (50 µM)	449.5 ± 22.56	0.234 ± 0.250	+35.2 ± 1.39

Figure 3. Physicochemical characterization of **H_2-PG**/siRNA nanoparticles. (a) Gel electrophoresis analysis at N/P = 2, 5, and 10 showing the full complexation of siRNA by **H_2-PG** at N/P ≥ 5; (b) Particles size, polydispersity index (PDI*) and ζ-potential measurements for the complexes formed between **H_2-PG** and siRNA ("compounds") at N/P = 5 with varying concentrations of **H_2-PG** (5, 25, and 50 µM). The values represent the average of three replicates.

Cellular uptake

Cellular uptake of the complex was evaluated in MDA-MB-231 cells by using confocal microscopy and flow cytometry. As shown in Figure 4, **H_2-PG** alone was able to get into the cells (red staining) and, more interestingly, it could also deliver the Atto-488-siCtrl into the cytoplasm (the yellow stain in the merged image was generated as a result of red (**H_2-PG**) and green (Atto-488-siRNA) fluorescence overlapping) as compared with Lipofectamine RNAiMax transfection. The free Atto-488 siCtrl itself did not enter cells since the Atto-488-siRNA fluorescence is observed around the plasma membrane in only few cells, thus proving that **H_2-PG** effectively transfect siRNA inside MDA-MB-231 cells.

In parallel, the cellular uptake of the **H_2-PG**/siRNA complex was quantified by flow cytometry which further proved that **H_2-PG** alone is able to quantitatively penetrate cells (Figure 5, lower left panel). The **H_2-PG**–siRNA complex is also able to penetrate cells, in which a significant part of **H_2-PG** (~23%) was associated with the siRNA (Figure 5, lower right panel). In contrast, with the naked siRNA, we observed only a weak

fluorescence signal (8%, Figure 5, upper middle panel) due to its adsorption to the plasma membrane as seen in confocal microscopy (Figure 4). We observed also an uptake with the lipofectamine siRNA transfection (Figure 5, upper right panel). However, as lipofectamine presents a cytotoxic effect, the transfected cells became apoptotic as revealed by Propidium Iodide (PI) staining (shown in cyan color in Figure 5).

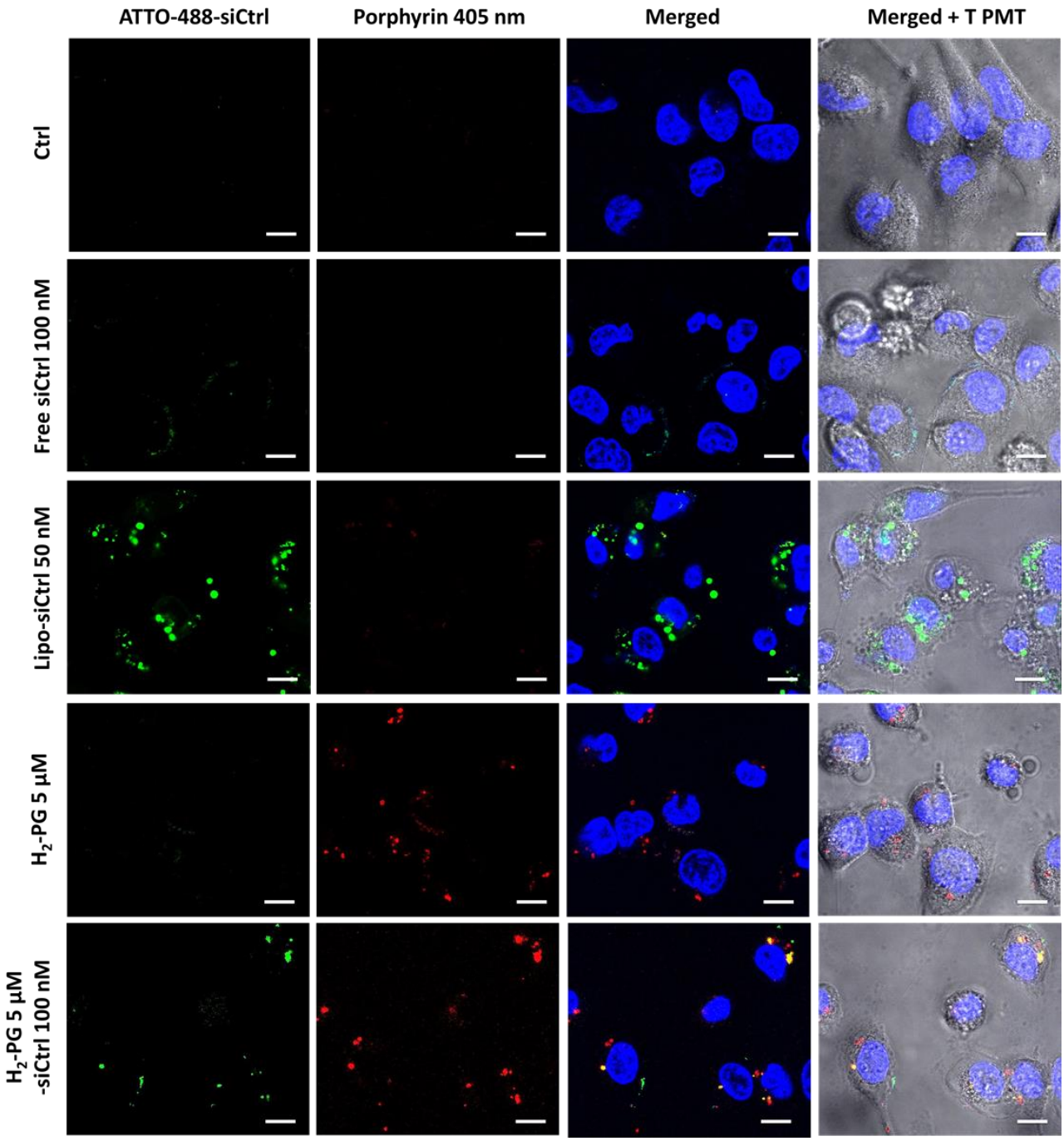

Figure 4. Cellular uptake of **H_2-PG**/siRNA complexes by MDA-MB-231 cells visualized by confocal microscopy. From the top to the bottom respectively: MDA-MB 231 cells alone, incubated with Atto-488-siCtrl at 100 nM, incubated with the complex formed between lipofectamine and siRNA at 50 nM, incubated with **H_2-PG** (5 µM) alone, and finally with the complex formed between **H_2-PG** (5 µM) and siRNA (100 nM) at N/P = 5. The blue fluorescence indicates the nuclei (Hoechst 33342), siCtrl appears in green, porphyrins appear in red. The yellow staining (lower panel) is obtained by the overlapping of **H_2-PG** (red) and siRNA (green). Scale bar = 10 µm.

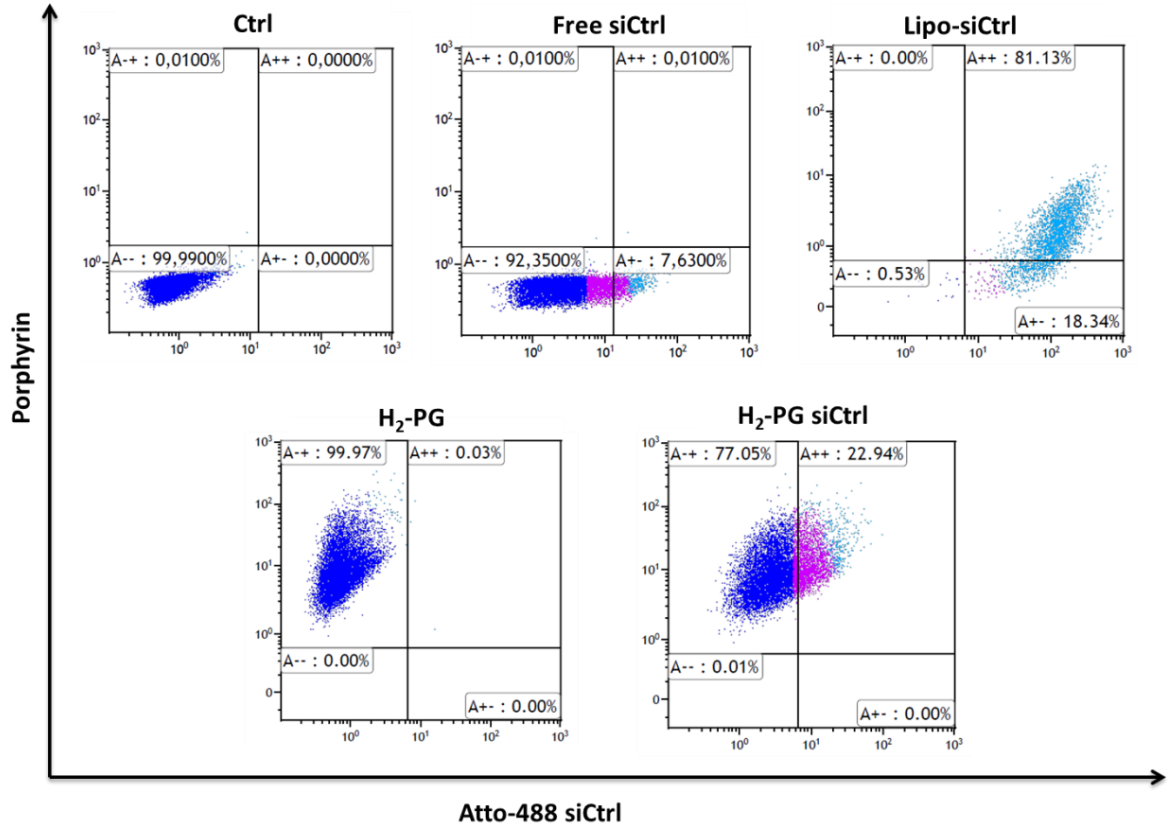

Figure 5. Cellular uptake quantified by flow cytometric analysis of MDA-MB-231 cells treated with **H_2-PG**/siRNA complexes. MDA-MB 231 cells alone (upper left), cells incubated with Atto-488-siCtrl (upper middle), cells incubated with the complex formed between lipofectamine and siRNA (upper right), cells incubated with **H_2-PG** alone (lower left) and finally, cells incubated with the complex formed between **H_2-PG** and siRNA at N/P = 5 (lower right). The cyan color indicates the apoptotic cells as revealed by propidium iodidestaining. Numbers in the profiles indicate the percentage of cells present in this area.

***In vitro* combined PDT and siRNA delivery**

For assessing the potential therapeutic use of **H_2-PG**/siRNA complex in PDT-siRNA combination therapy, we set up experiments using siRNA targeting the expression of proteins inhibitors of apoptosis (IAP). Indeed, Yang *et al.* reported that survivin, livin and inhibitors of apoptosis (IAP) are overexpressed in cancer cells and inhibit the apoptosis pathway.[40] For that we explored the mechanism of IAP, considering them as a group of proteins that make cancer cells insensitive to apoptosis.[41] MDA-MB 231 cells were treated with different concentrations of **H_2-PG** alone and **H_2-PG**/siIAP complex (N/P = 5), and cell viability was detected using an MTT assay, without or after light irradiation using a continuous laser at 405 nm for 10 min.

Without light irradiation, the cell viability was only slightly affected by the incubation with **H_2-PG** alone (Figure 6a), with still 75% cell viability at 25 µM concentration of **H_2-PG**. Although this "dark-cytotoxicity" (i.e. in the absence of light excitation) is not negligible, it remains acceptable and allowed us to further consider a biological use of **H_2-PG**. Still without light irradiation, incubation with**H_2-PG**/siIAP was satisfyingly found to knockdown IAP expression in a dose-dependent manner, lowering cell viability to 73% and 54% cell death at 5 µM and 25 µM, respectively (Figure 6a). In contrast, a much weaker effect was observed with a scramble siRNA (cell viability to 94% and 79% cell death at 5 µM and 25 µM, respectively (Figure 6a). Together with the imaging studies discussed above, and since cell viability was not affected when cells were incubated with siIAP alone, this experiment further demonstrates that **H_2-PG** acts as a delivery vehicle for siRNA which otherwise does not readily enter cells.

Following light irradiation (405 nm, 10 min) of the cells incubated with **H_2-PG** alone, the cell viability was significantly decreased – to 50% and 35% at, respectively, 5 µM and 25 µM (Figure 6a) – compared to the experiment without light irradiation or those without **H_2-PG**, thereby evidencing the PDT effect of **H_2-PG**.
Finally, cells incubated with **H_2-PG**/siIAP complex followed by light irradiation showed the lowest cell viability – 37% and 26% at, respectively, 5 µM and 25 µM (Figure 6a) – thus demonstrating the advantage of combining the two therapies, PDT and gene silencing, and validating our supramolecular approach to this quest.
To further investigate the combined effect of the two therapies, the results were subjected to data treatment using CompuSyn software (ComboSyn, Inc),[42] which yield combination indexes (CI) lower than 1 in case of synergistic interactions, equal to 1 in case of additive interactions, and greater than 1 in case of antagonist interactions.[42] In our case, CI were found to be around a value of 1 (Figure 6b), meaning that PDT acted additively with gene silencing in producing cytotoxicity in MDA-MB-231 cells.
The fact that synergism does not take place in our case would mean that the two therapies operate in parallel rather than sequentially. Therefore photochemical internalization[3] and photo-induced endosomal release[4] do not seem to take place in the present case. However, it is noteworthy to mention that achieving an additive effect is already a very positive result. Indeed, one could have feared that if **H_2-PG** remains too closely bound to siRNA, light irradiation would lead to the photo-degradation of the latter, thereby leading to an antagonist effect. In addition, aggregates of porphyrins are usually less active photosensitizers than molecularly-dispersed porphyrins. Thus, we believe that the obtained results indicate that **H_2-PG** releases from the **H_2-PG**/siRNA complex following cell internalization and thus enables the two therapies to occur effectively in an additive manner.

(a)

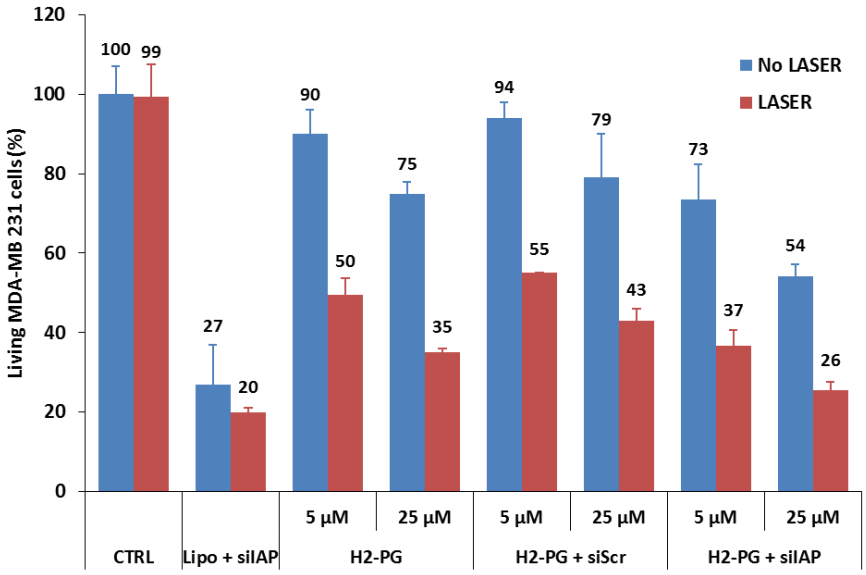

(b)

Concentrations (µM)	CI*
5.0	1.03
10.0	0.99
20.0	1.22
25.0	1.15

Figure 6. *In vitro* combination of PDT and siIAP delivery using **H_2-PG**. (a) Cell counting % of living MDA-MB-231 cells (MTT assay) treated with **H_2-PG** alone, **H_2-PG**/siScr complex at N/P = 5, **H_2-PG**/siIAP complex at N/P = 5, using two different concentrations of **H_2-PG** (5 and 25 µM) and siRNA (100 nM and 500 nM, respectively), with and without light irradiation (photon excitation laser at 405 nm for 10 min). Data are presented as (mean ± SEM). Experiments were carried out in triplicates; (b)report table of combination indexes obtained by data treatment using CompuSyn software. *Combination index (CI) was calculated from the CI equation algorithms using CompuSyn software. CI = 1, <1, and >1 indicates additive effect, synergism, and antagonism, respectively.

Gene silencing

To further test the specificity and efficiency of the silencing effects of **H_2-PG**/siRNA complexes on IAP protein expression, MDA-MB-231 cells were incubated with different complexes or with **H_2-PG** and siRNA separately. MDA-MB-231 cells were also transfected with a complex formed between lipofectamine and siRNA used as a positive control. In-cell ELISA was then used to measure the decrease of IAP expression following treatment of MDA-MB-231 cells with different formulations. Cells treated with media only in the absence of siRNA showed normal IAP expression before (100%) and after (99%) irradiation (Figure 7, Ctrl). The cells treated with naked siIAP gave the same level of IAP expression (108% for non-irradiated and 92% for irradiated cells) compared to the control (Figure 7, Free siIAP) The silencing of IAP expression was more pronounced when cells were treated with **H_2-PG**–siIAP complexes, resulting in an average of 42% (non-irradiated) and 57% (irradiated) decrease in protein expression (Figure 6, H_2-PG + siIAP). In contrast, the complexes formed between **H_2-PG** and a scrambled siRNA (siScr) had a much weaker effect on protein expression (20% inhibition for non-irradiated and 32% for irradiated cells) (Figure 7, H_2-PG + siScr). In comparison, cells transfected with siIAP using Lipofectamine decreased the protein expression by 50 % (non-irradiated) and 43% (irradiated) (Figure 7, Lipo + siIAP). Altogether, the protein quantification by in-cell ELISA experiment showed the efficiency of the **H_2-PG**/siRNA complex for gene silencing of therapeutic target such as IAP protein.

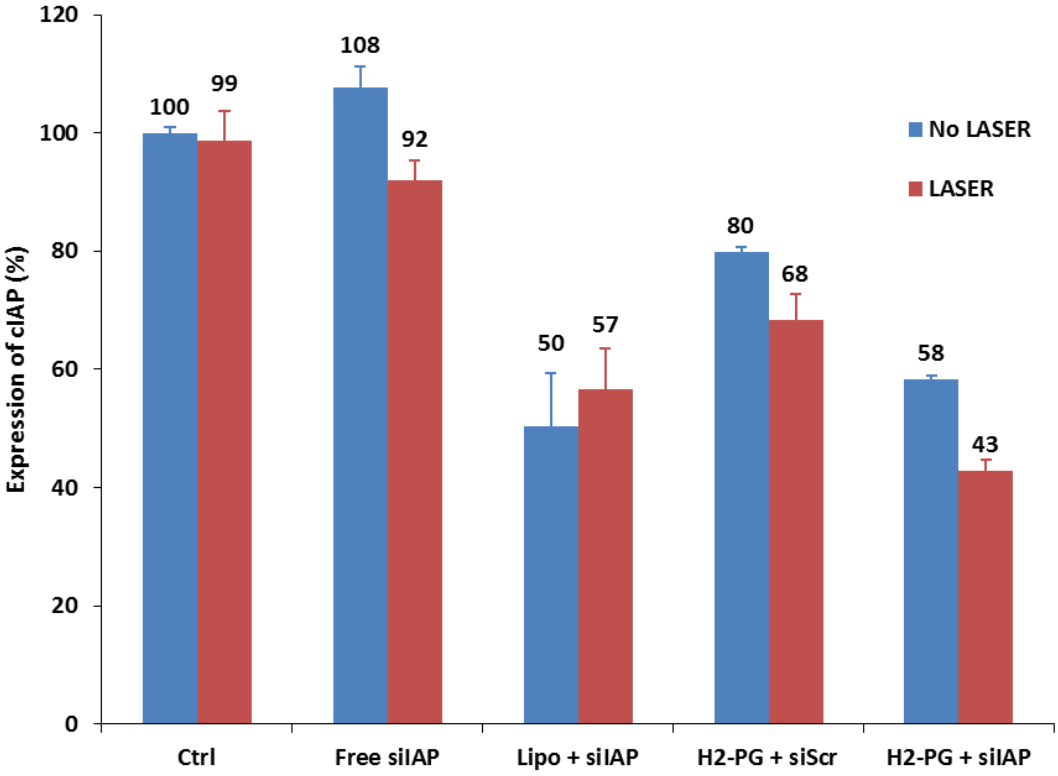

Figure 7. Silencing of IAP protein expression in MDA-MB-231 cells treated with different siRNA formulations. In-cell ELISA of IAP protein expression in MDA-MB-231 cells alone (Ctrl) using an anti-IAP antibody, in cells treated with naked siIAP (Free siIAP, 500 nM), in cells transfected with lipofectamine and siIAP (Lipo + siIAP, 50 nM), cells treated with a complex formed between **H_2-PG** and a scrambled siRNA (**H_2-PG**, 25 µM + siScr, 500 nM) and finally cells treated with **H_2-PG**/siIAP complex (**H_2-PG**, 25 µM + siIAP, 500 nM). In-cell ELISA was done with two different cell populations, non-irradiated (blue bars) and irradiated at 405 nm for 10 min (red bars). Experiments were carried out in triplicates. Data are presented as mean ± SEM.

Conclusions

We described here a supramolecular approach to achieve the combination of photodynamic therapy and gene therapy using a simple cationic porphyrin. Through this work, the guanidylated porphyrin **H_2-PG** was shown to interact with nucleic acids, yielding DNA-templated supramolecular polymers with ssDNA, more complicated association complexes with dsDNA, and nanoparticles of 200-500 nm diameter in presence of siRNA. We showed that **H_2-PG** readily enters human breast cancer cells (MDA-MB-231), and, more importantly, that it is able to act as a delivery vehicle to deliver siRNA inside cells, while retaining its PDT activity as a photosensitizer. Finally, thanks to this dual role of delivery vector and photosensitizer of **H_2-PG**, we succeeded in demonstrating an additive effect of PDT and siRNA therapy in living cells. Given the tremendous progresses recently made in the design of novel photosensitizers (with two-photon excitation, absorption in the near infra-red, etc…), we believe this proof-of-concept can open further perspectives in exploiting supramolecular self-assembly processes for therapeutic purposes.[43] The combined effect of PDT and gene silencing is of great interest for cancer therapy since it was already demonstrated that the PDT acts positively to impede the Epithelial-Mesenchymal transition (EMT) process in cancer cells.[44] To go further with this study, a challenge that now lies ahead is to insert a targeting motif to the **H_2-PG** vector for *in vivo* application, so that the targeted vector could become suitable for intravenous injection to deliver the siRNA into tumor for combined PDT and gene therapy.

Author contributions

NL, MC, LL, and YB: experimental research; CB, NB, and SU: designed project; MGB, GP, CB, NB, SU: results analysis and project management; NB, SU: funding acquisition and manuscript writing. All authors reviewed the manuscript.

Funding

This work was supported by the ANR (ANR-17-CE07-0042-01) and the Ligue Nationale contre le Cancer, section Hérault (2019).

Declaration of interest

The authors declare no conflicts of interest.

Acknowledgements

NL thanks the Ministère Algérien de l'Enseignement Supérieur et de la Recherche Scientifique for a PhD fellowship. The authors thank MRI (Montpellier RIO Imaging platform) for confocal microscopy facilities.

References

[1] Cancer: an old disease, a new disease or something in between?, A. R. David, M. R. Zimmerman, *Nat. Rev. Cancer*, **2010**, *10*, 728 (Doi: 10.1038/nrc2914).

[2] "Combo" nanomedicine: Co-delivery of multi-modal therapeutics for efficient, targeted, and safe cancer therapy, J. A. Kemp, M. S. Shim, C. Y. Heo, Y. J. Kwon, *Adv. Drug Deliv. Rev.*, **2016**, *98*, 3 (Doi: 10.1016/j.addr.2015.10.019).

[3] Non-toxic phototriggered gene transfection by PAMAM-porphyrin conjugates, M. J. Shieh, C. L. Peng, P. J. Lou, C. H. Chiu, T. Y. Tsai, C. Y. Hsu, C. Y. Yeh, P. S. Lai, *J. Control. Release*, **2008**, *129*, 200 (Doi: 10.1016/j.jconrel.2008.03.024).

[4] Dynamics of photoinduced endosomal release of polyplexes, K. G. de Bruin, C. Fella, M. Ogris, E. Wagner, N. Ruthardt, C. Brauchle, *J. Control. Release*, **2008**, *130*, 175 (Doi: 10.1016/j.jconrel.2008.06.001).

[5] Safety, Tolerability, and Pharmacokinetics of ARC-520 Injection, an RNA Interference-Based Therapeutic for the Treatment of Chronic Hepatitis B Virus Infection, in Healthy Volunteers, T. Schluep,

J. Lickliter, J. Hamilton, D. L. Lewis, C. L. Lai, J. Y. N. Lau, S. A. Locarnini, R. G. Gish, B. D. Given, *Clin. Pharmacol. Drug Dev.*, **2017**, *6*, 350 (Doi: 10.1002/cpdd.318).

[6] Preclinical Mammalian Safety Studies of EPHARNA (DOPC Nanoliposomal EphA2-Targeted siRNA), M. J. Wagner, R. Mitra, M. J. McArthur, W. Baze, K. Barnhart, S. Y. Wu, C. Rodriguez-Aguayo, X. N. Zhang, R. L. Coleman, G. Lopez-Berestein, A. K. Sood, *Mol. Cancer Ther.*, **2017**, *16*, 1114 (Doi: 10.1158/1535-7163.MCT-16-0541).

[7] Phase I clinical development of Atu027, a siRNA formulation targeting PKN3 in patients with advanced solid tumors, D. Strumberg, B. Schultheis, U. Traugott, C. Vank, A. Santel, O. Keil, K. Giese, J. Kaufmann, J. Drevs, *Int. J. Clin. Pharmacol. Ther.*, **2012**, *50*, 76 (Doi: 10.5414/CPP50076).

[8] Photodynamic therapy for cancer, D. E. J. G. J. Dolmans, D. Fukumura, R. K. Jain, *Nat. Rev. Cancer*, **2003**, *3*, 380 (Doi: 10.1038/Nrc1071).

[9] Porphyrinoid biohybrid materials as an emerging toolbox for biomedical light management, V. Almeida-Marrero, E. van de Winckel, E. Anaya-Plaza, T. Torres, A. de la Escosura, *Chem. Soc. Rev.*, **2018**, *47* (Doi: 10.1039/c7cs00554g).

[10] The role of porphyrin chemistry in tumor imaging and photodynamic therapy, M. Ethirajan, Y. H. Chen, P. Joshi, R. K. Pandey, *Chem. Soc. Rev.*, **2011**, *40*, 340 (Doi: 10.1039/b915149b).

[11] Ultrasound-targeted photodynamic and gene dual therapy for effectively inhibiting triple negative breast cancer by cationic porphyrin lipid microbubbles loaded with HIF1 alpha-siRNA, S. J. Sun, Y. X. Xu, P. Fu, M. Chen, S. H. Sun, R. R. Zhao, J. R. Wang, X. L. Liang, S. M. Wang, *Nanoscale*, **2018**, *10*, 19945 (Doi: 10.1039/c8nr03074j).

[12] The potential of photodynamic therapy (PDT)-Experimental investigations and clinical use, A. Oniszczuk, K. A. Wojtunik-Kuleszaa, T. Oniszczuk, K. Kasprzak, *Biomed. Pharmacother.*, **2016**, *83*, 912 (Doi: 10.1016/j.biopha.2016.07.058).

[13] Advanced Photosensitizer Activation Strategies for Smarter Photodynamic Therapy Beacons, B. M. Luby, C. D. Walsh, G. Zheng, *Angew. Chem. Int. Ed.*, **2019**, *58*, 2558 (Doi: 10.1002/anie.201805246).

[14] Supramolecular photosensitizers rejuvenate photodynamic therapy, X. Li, S. Lee, J. Yoon, *Chem. Soc. Rev.*, **2018**, *47*, 1174 (Doi: 10.1039/c7cs00594f).

[15] Bimodal Targeting Using Sulfonated, Mannosylated PEI for Combined Gene Delivery and Photodynamic Therapy, U. Chitgupi, Y. Li, M. F. Chen, S. Shao, M. Beitelshees, M. J. Tan, S. Neelamegham, B. A. Pfeifer, C. Jones, J. F. Lovell, *Photochem. Photobiol.*, **2017**, *93*, 600 (Doi: 10.1111/php.12688).

[16] Porous Porphyrin-Based Organosilica Nanoparticles for NIR Two-Photon Photodynamic Therapy and Gene Delivery in Zebrafish, C. M. Jimenez, D. Aggad, J. G. Croissant, K. Tresfield, D. Laurencin, D. Berthomieu, N. Cubedo, M. Rossel, S. Alsaiari, D. H. Anjum, R. Sougrat, M. A. Roldan-Gutierrez, S. Richeter, E. Oliviero, L. Raehm, C. Charnay, X. Cattoen, S. Clement, M. W. C. Man, M. Maynadier, V. Chaleix, V. Sol, M. Garcia, M. Gary-Bobo, N. M. Khashab, N. Bettache, J. O. Durand, *Adv. Funct. Mat.*, **2018**, *28*, Artn 1800235 (Doi: 10.1002/Adfm.201800235).

[17] Supramolecular nanocarriers integrated with dendrimers encapsulating photosensitizers for effective photodynamic therapy and photochemical gene delivery, N. Nishiyama, W. D. Jang, K. Kataoka, *New J. Chem.*, **2007**, *31*, 1074 (Doi: 10.1039/b616050f).

[18] Co-delivery of anti-PLK-1 siRNA and camptothecin by nanometric polydiacetylenic micelles results in a synergistic cell killing, M. Ripoll, M. Pierdant, P. Neuberg, D. Bagnard, A. Wagner, A. Kichler, J. S. Remy, *RSC Adv.*, **2018**, *8*, 20758 (Doi: 10.1039/c8ra03375g).

[19] Photo-Induced Charge-Variable Conjugated Polyelectrolyte Brushes Encapsulating Upconversion Nanoparticles for Promoted siRNA Release and Collaborative Photodynamic Therapy under NIR Light Irradiation, H. Zhao, W. B. Hu, H. H. Ma, R. C. Jiang, Y. F. Tang, Y. Ji, X. M. Lu, B. Hou, W. X. Deng, W. Huang, Q. L. Fan, *Adv. Func. Mat.*, **2017**, *27*, Artn 1702592 (Doi: 10.1002/Adfm.201702592).

[20] From self-assembly to noncovalent synthesis of programmable porphyrins' arrays in aqueous solution, A. D'Urso, M. E. Fragala, R. Purrello, *Chem. Commun.*, **2012**, *48*, 8165 (Doi: 10.1039/c2cc31856c).

[21] Bioactive clusters promoting cell penetration and nucleic acid complexation for drug and gene delivery applications: from designed to self-assembled and responsive systems, E. Bartolami, C. Bouillon, P. Dumy, S. Ulrich, *Chem. Commun.*, **2016**, *52*, 4257 (Doi: 10.1039/c5cc09715k).

[22] The nickel(II) complex of guanidinium phenyl porphyrin, a specific G-quadruplex ligand, targets telomeres and leads to POT1 mislocalization in culture cells, L. Sabater, M. L. Nicolau-Travers, A. De

Rache, E. Prado, J. Dejeu, O. Bombarde, J. Lacroix, P. Calsou, E. Defrancq, J. L. Mergny, D. Gomez, G. Pratviel, *J. Biol. Inorg. Chem.*, **2015**, *20*, 729 (Doi: 10.1007/s00775-015-1260-8).
[23] A Dynamic Combinatorial Approach for Identifying Side Groups that Stabilize DNA-Templated Supramolecular Self-Assemblies, D. Paolantoni, S. Cantel, P. Dumy, S. Ulrich, *Int. J. Mol. Sci.*, **2015**, *16*, 3609 (Doi: 10.3390/ijms16023609).
[24] Probing the importance of π-stacking interactions in DNA-templated self-assembly of bisfunctionalized guanidinium compounds, D. Paolantoni, J. Rubio-Magnieto, S. Cantel, J. Martinez, P. Dumy, M. Surin, S. Ulrich, *Chem. Commun.*, **2014**, *50*, 14257 (Doi: 10.1039/C4CC05706F).
[25] Synthesis of asymmetric guanidiniumphenyl-aminophenyl porphyrins, A. Perrier, E. Mothes, C. Bonduelle, G. Pratviel, *J. Porphyr. Phthalocya.*, **2016**, *20*, 1438 (Doi: 10.1142/S1088424616501170).
[26] The commonly used N/P ratio refers to the number of positive charges brought by the H2-PG vector divided by the number of negative charges brought by the nucleic acid.
[27] Porphyrins in complex with DNA: Modes of interaction and oxidation reactions, G. Pratviel, *Coord. Chem. Rev.*, **2016**, *308*, 460 (Doi: 10.1016/j.ccr.2015.07.003).
[28] Click Modification of Diazido Acridine Intercalators: A Versatile Route towards Decorated DNA Nanostructures, S. M. Hafshejani, S. M. D. Watson, E. M. Tuite, A. R. Pike, *Chem. Eur. J.*, **2015**, *21*, 12611 (Doi: 10.1002/chem.201501836).
[29] Synthesis and binding of proflavine diazides as functional intercalators for directed assembly on DNA, S. MoradpourHafshejani, J. H. Hedley, A. O. Haigh, A. R. Pike, E. M. Tuite, *RSC Adv.*, **2013**, *3*, 18164 (Doi: 10.1039/c3ra43090a).
[30] DNA-templated assembly of helical cyanine dye aggregates: A supramolecular chain polymerization, K. C. Hannah, B. A. Armitage, *Acc. Chem. Res.*, **2004**, *37*, 845 (Doi: 10.1021/ar030257c).
[31] DNA-templated formation of a helical cyanine dye J-aggregate, M. M. Wang, G. L. Silva, B. A. Armitage, *J. Am. Chem. Soc.*, **2000**, *122*, 9977 (Doi: 10.1021/Ja002184n).
[32] Porphyrin - Nucleic-Acid Interactions - a Review, R. J. Fiel, *J. Biomol. Struct. Dyn.*, **1989**, *6*, 1259 (Doi: 10.1080/07391102.1989.10506549).
[33] Intercalative and Nonintercalative Binding of Large Cationic Porphyrin Ligands to Calf Thymus DNA, M. J. Carvlin, R. J. Fiel, *Nucleic Acids Res.*, **1983**, *11*, 6121 (Doi: 10.1093/nar/11.17.6121).
[34] Interaction of DNA with a Porphyrin Ligand - Evidence for Intercalation, R. J. Fiel, J. C. Howard, E. H. Mark, N. Dattagupta, *Nucleic Acids Res.*, **1979**, *6*, 3093 (Doi: 10.1093/Nar/6.9.3093).
[35] From nucleobase to DNA templates for precision supramolecular assemblies and synthetic polymers, M. Surin, *Polym. Chem.*, **2016**, *7*, 4137 (Doi: 10.1039/c6py00480f).
[36] Internal Versus External Binding of Cationic Porphyrins to Single-Stranded DNA, A. J. Gaier, S. Ghimire, S. E. Fix, D. R. McMillin, *Inorg. Chem.*, **2014**, *53*, 5467 (Doi: 10.1021/ic403105q).
[37] ssDNA templated self-assembly of chromophores, P. G. A. Janssen, J. Vandenbergh, J. L. J. van Dongen, E. W. Meijer, A. P. H. J. Schenning, *J. Am. Chem. Soc.*, **2007**, *129*, 6078 (Doi: 10.1021/Ja0711967).
[38] Circular dichroism to determine binding mode and affinity of ligand-DNA interactions, N. C. Garbett, P. A. Ragazzon, J. B. Chaires, *Nature Prot.*, **2007**, *2*, 3166 (Doi: 10.1038/nprot.2007.475).
[39] Cationic Copper(II) Porphyrins Intercalate into Domains of Double-Stranded RNA, B. N. Briggs, A. J. Gaier, P. E. Fanwick, D. K. Dogutan, D. R. McMillin, *Biochemistry*, **2012**, *51*, 7496 (Doi: 10.1021/bi300828z).
[40] Therapeutic potential of siRNA-mediated combined knockdown of the IAP genes (Livin, XIAP, and Survivin) on human bladder cancer T24 cells, D. Y. Yang, X. S. Song, J. N. Zhang, L. Ye, S. J. Wang, X. Y. Che, J. B. Wang, Z. W. Zhang, L. N. Wang, W. Shi, *Acta Biochim. Biophys. Sin.*, **2010**, *42*, 137 (Doi: 10.1093/abbs/gmp118).
[41] Inhibitor of apoptosis proteins and apoptosis, Y. B. Wei, T. J. Fan, M. M. Yu, *Acta Biochim. Biophys. Sin.*, **2008**, *40*, 278 (Doi: 10.1111/j.1745-7270.2008.00407.x).
[42] Theoretical basis, experimental design, and computerized simulation of synergism and antagonism in drug combination studies, T. C. Chou, *Pharmacol. Rev.*, **2006**, *58*, 621 (Doi: 10.1124/pr.58.3.10).
[43] Growing Prospects of Dynamic Covalent Chemistry in Delivery Applications, S. Ulrich, *Acc. Chem. Res.*, **2019**, *52*, 510 (Doi: 10.1021/acs.accounts.8b00591).
[44] Nanoparticle delivery of Wnt-1 siRNA enhances photodynamic therapy by inhibiting epithelial-mesenchymal transition for oral cancer, C. A. Ma, L. L. Shi, Y. Huang, L. Y. Shen, H. Peng, X. Y. Zhu, G. Y. Zhou, *Biomater. Sci.*, **2017**, *5*, 494 (Doi: 10.1039/c7bm90004j).